

Cardiac Magnetic Resonance Elastography

Toward the Diagnosis of Abnormal Myocardial Relaxation

Thomas Elgeti, MD,* Mark Beling, MD,† Bernd Hamm, MD,* Jürgen Braun, PhD,‡ and Ingolf Sack, PhD*

Aim: To assess the potential of cardiac magnetic resonance elastography (MRE) for elasticity-based detection of abnormal left ventricular (LV) relaxation.

Materials and Methods: Cardiac MRE was performed in 3 groups: young volunteers (n = 11; mean age, 31.7 years), older volunteers (n = 5; mean age, 54.8 years), and a group with relaxation abnormalities (n = 11; mean age, 58 years) identified by transthoracic echocardiography. Cine MR imaging served to measure LV volumes and global LV systolic function. Wave-amplitude-sensitive electrocardiograph-gated steady-state MRE was performed using an extended piston driver attached to the anterior chest wall. Phase contrast shear wave images were acquired in all 3 Cartesian components and combined to generate amplitude maps. This was done using the time-gradient operator for linear high-pass filtering and phase unwrapping followed by temporal Fourier transformation for extracting externally induced 24.13-Hz shear oscillations from intrinsic motion and blood flow. Amplitudes were evaluated in the left ventricle and normalized by wave amplitudes outside the heart, adjacent to the right ventricle.

Results: One patient and 1 young volunteer had to be excluded from final analysis because of considerable body movement during the acquisition of the MRE scans. Mean wave amplitudes in the remaining subjects were 0.22 ± 0.05 mm in young volunteers, 0.23 ± 0.09 in older volunteers, and 0.14 ± 0.03 mm in patients. The mean ratio of amplitudes inside the ventricle to the anterior chest wall was 0.62 ± 0.15 for young volunteers, 0.50 ± 0.09 for older volunteers, and 0.33 ± 0.08 for patients.

Conclusion: MRE identifies significantly reduced LV shear wave amplitudes in patients with mild relaxation abnormality. Thus, cardiac MRE provides a promising modality for an elasticity-based diagnosis of dysfunctional myocardial relaxation.

Key Words: cardiac MR elastography, relaxation abnormalities, diastolic dysfunction

(Invest Radiol 2010;45: 000–000)

Heart failure is associated with a significant morbidity, mortality, and financial burden to the health services.¹ About 50% of cases of cardiac failure mainly involve the diastolic part of the cardiac cycle.² In clinical routine, diastolic function is assessed using transthoracic echocardiography.³ Patients with diastolic dysfunction have increased myocardial stiffness, which is suggested by theoretical considerations and confirmed by observations in vivo and in vitro.^{4,5} Careful and definite diagnosis of diastolic dysfunction requires the measurement of pressure time curves⁶ because routine

assessment of diastolic filling by measurement of mitral flow can miss about 30% of the patients with diastolic dysfunction.³ A more practical approach is to determine tissue Doppler-derived indices, which are less prone to errors.⁷ Nevertheless, echocardiography can be challenging in obese patients or patients with a poor acoustic window.⁸ All current noninvasive imaging techniques may provide images with excellent spatial and temporal resolution but provide no direct measure of intramyocardial forces determined by the alteration of the heart's shear modulus. Cardiac magnetic resonance elastography (MRE) is a relatively new method to measure the time-varying cardiac shear modulus, a measure of cardiac stiffness, by application of low-frequency acoustic waves. Until now, this method has only been performed in animals and healthy volunteers.^{9–11}

The aim of the current study was to investigate the technical feasibility of cardiac MRE in patients with mild diastolic dysfunction diagnosed by transthoracic echocardiography and tissue Doppler-derived indices and compare the findings with those in a group of healthy volunteers.

We hypothesized that myocardial shear wave amplitude, a measure for the elastic shear modulus,¹¹ is lower in patients with diastolic dysfunction than in normal volunteers.

MATERIALS AND METHODS

Subjects

The study was approved by the local ethics committee (EA 1/055/07–4), and written informed consent was obtained from all subjects. A total of 11 patients with echocardiographically proven relaxation abnormalities (the criteria for diastolic dysfunction are defined in the following sections) were examined by standard cardiac magnetic resonance imaging (MRI) using a cine steady-state free precession sequence and cardiac MRE. Echocardiography, MRI, and MRE were also used in 16 controls (11 young and 5 older ones) with normal values for systolic and diastolic function and without a history of cardiac dysfunction.

Echocardiography

Transthoracic echocardiography was performed using standard methodology according to the recommendations of the American Society of Echocardiography (using Vivid 7 ultrasound system with an M3S transducer [1.5–4.0 MHz], GE Vingmed, Horton, Norway). The following echo variables were measured or derived: left ventricular (LV) dimensions, volumes, ejection fraction, left atrial dimensions, peak transmitral valve (MV) early diastolic (E) velocity, the average of septal and lateral myocardial annular tissue velocity (E'), the E/E' ratio, and the MV E/A ratio, where A is peak late diastolic transmitral velocity. Peak early and late diastolic transmitral velocities were measured using the pulsed Doppler technique, with the sample volume placed at level of the mitral leaflet tips during diastole in the apical 4-chamber view. The septal and lateral myocardial annular tissue velocities were recorded with the pulsed Doppler sample volumes positioned within 1 cm of the septal and lateral insertion sites of the mitral leaflets. Diastolic function was classified according to the criteria proposed by Nagueh

Received January 4, 2010; accepted for publication, after revision, May 29, 2010. From the Departments of *Radiology and †Cardiology, Angiology, and Pulmonology, Charité–Universitätsmedizin Berlin, Campus Mitte, Berlin, Germany; and ‡Institute of Medical Informatics, Charité–Universitätsmedizin Berlin, Campus Benjamin Franklin, Berlin, Germany.

Thomas Elgeti and Mark Beling contributed equally to this manuscript.

Supported by the German Research Foundation (DFG) Sa 901/3.

Reprints: Thomas Elgeti, MD, Department of Radiology, Charité–Universitätsmedizin Berlin, Campus Mitte, Charitéplatz 1, 10117 Berlin, Germany. E-mail: thomas.elgeti@charite.de.

Copyright © 2010 by Lippincott Williams & Wilkins

ISSN: 0020-9996/10/4512-0001

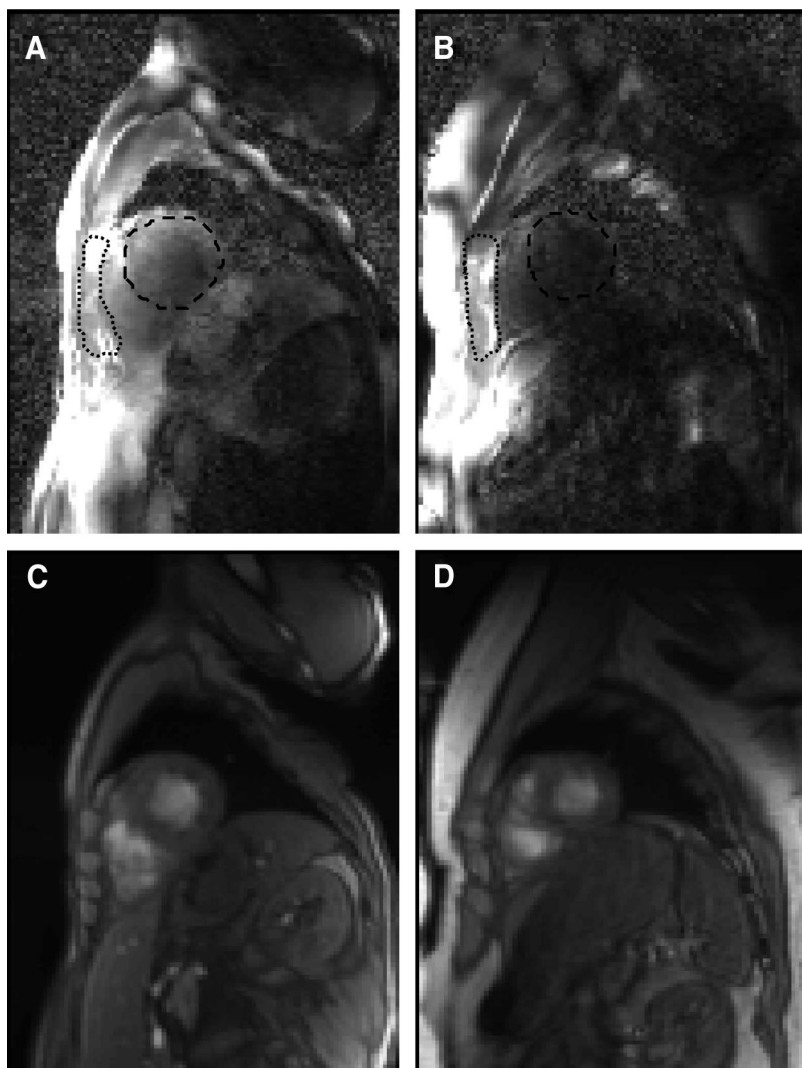


FIGURE 1. A, Image showing the wave amplitudes resulting from 24.13-Hz vibration of the anterior chest wall in a healthy volunteer. B, Image showing the wave amplitudes resulting from 24.13-Hz vibration of the anterior chest wall in a patient. The ROIs of LV and anterior chest wall (LV/REF) are indicated by dashed and dotted lines, respectively. The gray scale window of the amplitude maps is between 0 and 0.5 mm. A lower wave intensity in the left ventricle of the patient is clearly visible, although the intensity in the anterior chest wall appears similar to that of the healthy age-matched volunteer. C and D, The summed magnitude images of the experiments used for anatomic delineation of the left ventricle and in the anterior chest wall ROI: (C) volunteers, (D) patients.

et al¹² assuming abnormal function for MV E/A ratio <0.8 , absolute septal tissue velocity (sep E') <0.08 , and/or E/ E' ratio >8 .

Cardiac MRI

Cardiac MRI was performed on a clinical 1.5 T scanner (Siemens Avanto). LV volumes and function were assessed by means of retrospectively electrocardiograph (ECG)-gated cine steady-state free precession sequences: after piloting, sequences were run in the 3 doubly oblique long cardiac axes (slice thickness 5 mm, typical field of view [FoV] 370×310 mm, time of repetition [TR] 46.5 milliseconds, echo time [TE] 1.6 milliseconds, and matrix 256×160) and in the LV short axis (slice thickness 8 mm, typical FoV 320×240 mm, TR 40.7 milliseconds, TE 1.3 milliseconds, and matrix 192×144 , acceleration factor 2 [integrated parallel acquisition technique, generalized autocalibrating partially parallel acquisitions (GRAPPA)] in multiple slices [gap between the slices: 2 mm] to cover the whole left ventricle}.

Cardiac MRE

Cardiac MRE was performed after routine MRI in a short cardiac axis in the anterior third of the left ventricle using a method similar to that described in References 10 and 11. An ECG-gated gradient-recalled echo steady-state sequence (TR 5.18 milliseconds,

TE 3.29 milliseconds, flip angle = 25 degree, RF spoiling, 2-fold GRAPPA acceleration, 128×96 matrix, typical FoV 320×250 mm, 7 mm slice thickness, 48 single-line k -space segments, 1.3 kHz bandwidth) was sensitized to motion by a sinusoidal motion-encoding gradient (MEG) of $t = 2$ milliseconds duration corresponding to an MEG frequency of 500 Hz. Three MRE experiments were performed in each subject corresponding to different directions of the MEG along the Cartesian axes x_j of the image frame (given by the directions of read out [$j = 1$], phase encoding [$j = 2$], and slice selection [$j = 3$]). MEG amplitude g_j was 25 mT/m. The start of image acquisition was controlled by the R-wave of the ECG. A total of 360 identical k -lines were acquired, resulting in an observation time of cardiac function of approximately 1.86 seconds (TR $\times 360$). Images were reconstructed from 96 single-line k -space segments after 48 phase-encoding steps (96 k -lines, 75% phase sampling, GRAPPA factor 2 with 12 extra lines for image reconstruction). A delay of approximately 2.5 seconds after each phase-encoding step allowed respiration (eg, "controlled" breathing cycle). A customer-built actuator produced low-frequency acoustic vibrations, which were transferred to the patient's chest by a rigid piston.¹³ A sinusoidal burst of 24.13 Hz frequency (1/8TR) was fed into the actuator after each eighth TR, resulting in 45 (360/8) continuous harmonic

vibration cycles for each of the 48 phase-encoding steps. Depending on heart rate, 1 MRE scan for each MEG was acquired in approximately 3.5 to 4.0 minutes during controlled breathing.

MRE Data Processing

Raw phase images $\varphi(x, y, t) \in [0, 2\pi]$ were transformed to unwrapped phase-velocity images $\varphi Y(x, y, t) \in [-\infty, \infty]$ using the method proposed in Reference 11:

$$\frac{d\varphi}{dt} = -Ie^{-i\varphi} \frac{de^{i\varphi}}{dt} \tag{1}$$

The phase velocity $\dot{\varphi}$ represents linear frequency-filtered phase oscillations dominated by steady-state time-harmonic oscillations of frequency $f = 24.13$ Hz induced by the actuator. This time-harmonic phase-velocity is related to deflections (in microns) by

$$u_j = q \frac{\dot{\varphi}}{\omega} \text{ with } q = \left| \frac{\pi(1 - \tau^2 f^2)}{\gamma g_j \tau \sin(\pi N \tau f)} \right| \tag{2}$$

The factor q in units of micrometer per radians is the inverse of the encoding efficiency, as derived in one study,¹⁴ which includes all relevant terms of harmonic motion-sensitive MRI by sinusoidal MEGs: gradient direction (given by x_j), gradient strength (g_j), period time of the sinusoidal gradient (t), number of gradient periods ($N = 1$, in our case), drive frequency (f), and gyromagnetic ratio of the protons (γ). Each vibration component u_j was further Fourier-transformed in time, yielding 3 complex wave images at drive frequency $\hat{u}_j = \hat{u}_j(x, y, f)$ needed to calculate wave amplitude images for measuring the change in wave amplitudes. The magnitude of shear waves is given by $U = \sqrt{\hat{u}_1 \hat{u}_1^* + \hat{u}_2 \hat{u}_2^* + \hat{u}_3 \hat{u}_3^*}$, with asterisks denoting the complex conjugate. For low signals, ie, if the variance caused by noise exceeds signal amplitudes, the magnitude of the waves is determined by noise, giving rise to strongly overestimated wave amplitudes. This effect is reduced by considering

$$U = |\hat{u}'_1 + \hat{u}'_2 + \hat{u}'_3|/3, \tag{3}$$

as wave amplitude since each component \hat{u}'_j is an independent sample, which reduces noise before the magnitude. The prime in \hat{u}'_j denotes the pixel-wise phase-corrected wave image. Therefore, the phases of the complex signals in \hat{u}'_j were automatically rotated to yield a maximum of the real parts of \hat{u}'_j .

Because the transfer of shear wave energy through the thoracic wall is influenced by numerous physiological and experimental parameters determined by factors such as body weight, position of the transducer, vibration amplitude, a reference region was manually selected for normalizing the amplitudes encountered within the left ventricle. Therefore, we measured the shear wave amplitude in the following 2 regions of interest (ROIs): (i) the left ventricle (LV) and (ii) a reference region in the thoracic wall (REF) anterior to the right ventricle for specifying wave amplitudes before the waves enter the heart. Henceforth, wave amplitudes according to the ROI inside the left ventricle and the ROI in the chest wall are referred to as U_{LV} and U_{REF} , respectively. Figure 1 demonstrates the selection of ROIs in 1 volunteer (A) and 1 patient (C).

Statistics

Statistics were calculated by MATLAB (Version 7.0.4, The MathWork Inc.). Descriptive statistics are expressed as mean with standard deviation. The Wilcoxon test for 2 independent samples and Bonferroni post hoc correction was used to test U_{LV} and U_{REF}

TABLE 1. Patient Characteristics and Global Cardiac Parameters From Echocardiography, MRI, and Cardiac MRE*

Patient No. (F)	Age (yr)	BMI	History/Pathology	Echo			MRI LV (BSA)			MRE		
				MV E/A	sep E' (m/s)	E/E'	EDV (mL)	EF (%)	MM (g)	U_{LV} (mm)	U_{REF} (mm)	Ratio (U_{LV}/U_{REF})
1	63	31	HTN	0.679	0.07	8.1	51	63	70	0.14	0.50	0.28
2 (F)	69	33	HTN	0.625	0.06	8.3	54	58	53	0.13	0.47	0.27
3 (F)	63	28	HTN	0.74	0.05	14	56	70	66	0.13	0.48	0.26
4	48	31	HCM, HTN	0.74	0.05	7.8	65	70	97	0.14	0.40	0.34
5	61	25	HTN	0.6	0.07	8.6	68	61	69	0.18	0.44	0.41
6	44	28	HTN	0.75	0.07	11	58	55	72	0.16	0.33	0.47
7	67	32	HTN	0.74	0.03	10	91	35	97	0.10	0.40	0.25
8	48	27	Post myo-carditis	0.75	0.06	9.4	69	68	60	0.15	0.36	0.40
9	70	29	CAD	0.48	0.03	12	124	37	107	0.16	0.49	0.33
10	48	27	HTN	0.75	0.07	7.7	65	52	60	0.09	0.38	0.24
Mean \pm SD	58.1 \pm 10.0	28.9 \pm 2.8		0.69 \pm 0.09	0.06 \pm 0.01	9.7 \pm 2.1	70.1 \pm 22.0	56.9 \pm 12.6	75.1 \pm 18.5	0.14 \pm 0.03	0.43 \pm 0.06	0.33 \pm 0.08

*The mean age was 58 yr, as compared with normal the body weight was increased resulting in an increased body mass index (mean of 29). The echocardiographic values represent typical findings for relaxation abnormalities, indicating mild diastolic dysfunction. Except for 2 patients, systolic function was normal.
 sep E' indicates absolute septal velocity obtained by tissue Doppler; EDV, enddiastolic volume; EF, ejection fraction; MM, myocardial mass; HTN, hypertension; CAD, coronary artery disease; HCM, hypertrophic nonobstructive cardiomyopathy; f, female; MRI, magnetic resonance imaging; MRE, magnetic resonance elastography; SD, standard deviation; BMI, body mass index; BSA, body surface area; MV, peak transmitral valve; E/E', early diastolic velocity ratios.

TABLE 2. Characteristics, Epidemiologic, and Physiologic Parameters of the Control Groups*

Volunteer	Echo					MRI LV (/BSA)				MRE	
	Age (yr)	BMI	MV E/A	sep E' (m/s)	E/E'	EDV (mL)	EF (%)	MM (g)	U _{LV} (mm)	U _{REF} (mm)	Ratio (U _{LV} /U _{REF})
Younger volunteers (age range: 25–39 yr)											
11	38	26	1.4	0.13	5.38	74	62	72	0.17	0.30	0.56
12	39	20	2	0.15	4.1	60	65	50	0.21	0.41	0.51
13	31	25	1	0.16	4.0	90	68	85	0.24	0.31	0.79
14	36	25	1.4	0.12	5.83	85	70	54	0.21	0.22	0.94
15	28	20	1	0.12	4.1	81	61	83	0.23	0.33	0.72
16	33	23	2.5	0.16	5.0	67	62	59	0.28	0.52	0.54
17 (F)	34	20	1.3	0.14	3.8	68	60	55	0.32	0.62	0.51
18	26	26	2.5	0.15	7.0	54	65	68	0.15	0.31	0.50
19	27	23	1.2	0.16	4.0	60	58	60	0.17	0.28	0.61
20	25	21	1.0	0.13	3.9	75	63	62	0.24	0.38	0.63
Mean ± SD	31.7 ± 5.0	22.9 ± 2.5	1.5 ± 0.6	0.14 ± 0.02	4.71 ± 1.07	71.4 ± 11.7	63 ± 3.7	64.8 ± 12.0	0.22 ± 0.05	0.38 ± 0.14	0.62 ± 0.15
Older volunteers (age range: 47–59 yr)											
21	57	25	1.33	0.11	7.33	67	56	50	0.22	0.46	0.48
22 (F)	59	19	1.24	0.12	5.3	80	71	60	0.17	0.39	0.44
23 (F)	47	23	1.57	0.11	8.46	55	53	61	0.39	0.60	0.64
24	53	31	1.35	0.11	8.6	66	70	61	0.18	0.32	0.56
25 (F)	58	27	1.0	0.11	6.4	53	67	48	0.18	0.44	0.41
Mean ± SD	54.8 ± 4.9	25 ± 4.5	1.30 ± 0.21	0.11 ± 0.004	7.22 ± 1.4	64.2 ± 10.8	63.4 ± 8.3	56.0 ± 6.4	0.23 ± 0.09	0.44 ± 0.10	0.50 ± 0.09

*In the upper part of the table volunteers within the age range of 24–39 years, bottom part: age 47–59 years. Echocardiography/cardiac MRI showed normal parameters for left ventricular size and global systolic and diastolic function.
 sep E' indicates absolute septal velocity obtained by tissue Doppler; EDV, enddiastolic volume; EF, ejection fraction; MM, myocardial mass; HTN, hypertension; CAD, coronary artery disease; HCM, hypertrophic nonobstructive cardiomyopathy; F, female; MRI, magnetic resonance imaging; MRE, magnetic resonance elastography; SD, standard deviation; BMI, body mass index; BSA, body surface area; MV, peak transmitral valve; E/E', early diastolic velocity ratios.

and the resulting ratio for statistically significant differences. The level of significance was $P = 0.05$.

RESULTS

Experimental Procedures

In 1 patient and 1 volunteer considerable body movement was seen during the MRE experiment, resulting in a different short cardiac axis orientation and inconsistent LV ROI. These 2 subjects were excluded from further analysis.

Echocardiography

For simplicity, LV mass, volumes, and functional parameters are described under MRI in the Results section. All patients showed an altered mitral inflow pattern (MV E/A < 1, mean: 0.69 ± 0.09). The tissue Doppler-derived absolute septal velocities (sep E') were decreased (mean: 0.06 ± 0.01 m/s) and the myocardial early diastolic velocity ratios (E/E') ranged between 7.7 and 14, with a mean of 9.7 ± 2.1 . The 2 control groups showed normal echocardiographic findings (MV E/VA > 1, sep E' > 0.11 m/s, E/E' < 8). Echocardiographic parameters are displayed in Tables 1 (patients) and 2 (volunteers).

Cardiac MRI

LV size and function showed no significant differences in the mean volume indexed to body surface area between patients (70.1 mL) and control persons (young group 71.4 mL $P = 0.38$, old group 64.2 mL; $P = 0.84$). One patient with coronary artery disease (patient number 9) showed a significantly larger left ventricle (120 mL indexed to body surface area) compared with the normalized values of the remaining group. The systolic function of 2 patients was limited (EF of 35% and 37%). No significant difference of the mean was found in the global LV systolic function between patients (EF 56.5%) and controls (EF young group 63.4%, $P = 0.37$, older group 63.4%, $P = 0.31$). The LV myocardial mass was significantly larger in the patient group (75 g/m^2) compared with the age-matched control group (56 g/m^2 , $P = 0.04$), consistent with the history of hypertension in 8 patients. MRI-derived functional cardiac parameters are listed in Tables 1 and 2.

Cardiac MRE

Sequential vibration and controlled breathing were well tolerated by all subjects. Figure 1 illustrates the appearance of wave amplitude maps in a healthy volunteer and a patient. The relationship between tissue abnormality and MRE signal is demonstrated by the mean U_{LV} of all patients, which is 0.14 ± 0.03 mm and is significantly lower than that of the controls (0.22 ± 0.05 mm [$P < 0.01$] in the young group and 0.23 ± 0.09 mm [$P < 0.01$] in older controls). In contrast, the mean wave amplitude inside the anterior chest wall (U_{REF}) was similar in both groups (patients: 0.43 ± 0.06 mm; young controls: 0.38 ± 0.14 mm, [$P = 0.10$]; older controls 0.44 ± 0.10 mm [$P = 0.98$]). Therefore, the ratio (U_{LV}/U_{REF}) was used as diagnostic parameter for discriminating patients from volunteers. The mean amplitude ratio in patients was 0.33 ± 0.08 , which is clearly different from the mean ratio in healthy young volunteers of 0.62 ± 0.15 ($P < 0.001$) as well as the older volunteers 0.50 ± 0.09 mm ($P < 0.01$). Figure 2 shows box plots of the amplitude ratios in both groups. In this figure, the diagnostic threshold derived is 0.415, which was optimized for separating the group of patients from the age-matched controls.

DISCUSSION

In this study, for the first time we performed cardiac MRE in patients with mild (New York Heart Association class I) cardiac disease. Our experience shows that this method is applicable in

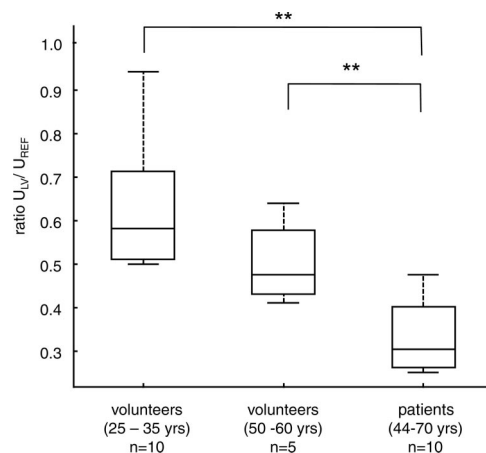


FIGURE 2. Box plot of the averaged shear wave amplitude ratios of LV/REF. The young (mean age, 31.7 years) and the old (mean age, 54.8 years) volunteers on the left and middle, the patient group (mean age, 58.1 years) on the right. The patient group with left ventricular relaxation abnormalities shows an effect on the externally induced shear wave amplitude ratio, which is significantly lower in patients: the lower and upper quartiles as well as the 50th percentile (median) are displayed. The full data range is represented by the whiskers. The shear wave amplitude ratios in the 2 control groups are not significantly different ($P = 0.1$).

patients. We propose a simple amplitude-based metric for assessing mechanical properties of the myocardium. Using the ratio U_{LV}/U_{REF} , we confirmed our hypothesis of reduced cardiac wave amplitudes in patients with impaired LV relaxation. Previous work in cardiac MRE focused either on the temporal variance of shear wave amplitudes⁹⁻¹¹ or on the appearance of wave patterns¹⁵⁻¹⁷ for deriving quantitative shear modulus values using specially designed inversion methods.¹⁸ Recent work in inversion-based cardiac MRE has shown the potential of applying this method to human beings.¹⁷ The method used here (ie, wave amplitude-sensitive MRE) was demonstrated in animals and humans beings to be capable of measuring time-resolved shear modulus variations related to ventricular pressure⁹ and cardiac pressure-volume work.¹⁰ Current technical developments in cardiac MRE need to focus on robust algorithms for extracting the diagnostic information carried by shear waves. In this respect, it is a very stimulating result of the present study that straightforward amplitude evaluation enables such a clear separation of patients and healthy volunteers. Because our analysis incorporates neither wave inversion nor time-dependent functional parameters, the proposed average of wave amplitudes is a most robust measure of the underlying mechanical properties of myocardial tissue. Yet, the results might be improved by involving time-resolved information, eg, about the duration of the phase of diastolic relaxation. For this reason, the results presented here should be seen as a first indication of the diagnostic potential of cardiac MRE. The aim of future work is to enable highly specific classification of elasticity parameters. In future studies, confounding factors such as body weight, gender, and age have to be addressed systematically. In this study, a preliminary estimation of age-dependent changes in cardiac physiology is given by presenting a limited subgroup of 5 elderly volunteers displaying slightly reduced amplitude ratios, U_{LV}/U_{REF} , compared with younger volunteers. However, because of the limited number of subjects, only a trend toward an amplitude reductions was observed ($P < 0.1$), which might be explained by an increased collagen content of myocardial tissue in elderly people.¹⁹ In this

respect, it is interesting to note that a further increase in myocardial collagen in chronic hypertension (the leading cause of diastolic dysfunction in the group investigated here) was measured,²⁰ which might explain the reduced shear wave amplitude ratios we found in patients and indicating an elevated myocardial elasticity level.

Two more challenges remain: First, 1 patient and 1 volunteer had to be excluded from final analysis because of considerable body movement during acquisition of the MRE scans for the 3 different vibration directions. With a total acquisition time of approximately 10 minutes (3×3.5 minutes per slice), there is a considerable risk that subjects will move. To overcome this drawback, we are currently working on a method that will allow acquisition of each scan in one breath-hold. It is expected, that acceptance and image quality of MRE will improve significantly. Second, although all subjects were imaged in a normal hydration state, significant changes in loading conditions of the heart—and therefore in the myocardial shear wave amplitude—cannot be ruled out.

Irrespective of these limitations, we conclude that cardiac MRE is a promising imaging-based modality for diagnosis of pathologically altered mechanical properties of the heart.

REFERENCES

1. Krum H, Abraham WT. Heart failure. *Lancet*. 2009;373:941–955.
2. Bleumink GS, Knetsch AM, Sturkenboom MC, et al. Quantifying the heart failure epidemic: prevalence, incidence rate, lifetime risk and prognosis of heart failure: the Rotterdam Study. *Eur Heart J*. 2004;25:1614–1619.
3. Kasner M, Westermann D, Steendijk P, et al. Utility of Doppler echocardiography and tissue Doppler imaging in the estimation of diastolic function in heart failure with normal ejection fraction: a comparative Doppler-conductance catheterization study. *Circulation*. 2007;116:637–647.
4. Zile MR, Baicu CF, Gaasch WH. Diastolic heart failure—abnormalities in active relaxation and passive stiffness of the left ventricle. *N Engl J Med*. 2004;350:1953–1959.
5. van Heerebeek L, Borbély A, Niessen HW, et al. Myocardial structure and function differ in systolic and diastolic heart failure. *Circulation*. 2006;113:1966–1973.
6. Kass DA. Assessment of diastolic dysfunction: invasive modalities. *Cardiol Clin*. 2000;18:571–586.
7. Nagueh SF, Middleton KJ, Kopelen HA, et al. Doppler tissue imaging: a noninvasive technique for evaluation of left ventricular relaxation and estimation of filling pressures. *J Am Coll Cardiol*. 1997;30:1527–1533.
8. Grothues F, Smith GC, Moon JC, et al. Comparison of interstudy reproducibility of cardiovascular magnetic resonance with two-dimensional echocardiography in normal subjects and in patients with heart failure or left ventricular hypertrophy. *Am J Cardiol*. 2002;90:29–34.
9. Elgeti T, Laule M, Kaufels N, et al. Cardiac MR elastography: comparison with left ventricular pressure measurement. *J Cardiovasc Magn Reson*. 2009;11:44.
10. Elgeti T, Rump J, Hamhaber U, et al. Cardiac magnetic resonance elastography: initial results. *Invest Radiol*. 2008;43:762–772.
11. Sack I, Rump J, Elgeti T, et al. MR elastography of the human heart: noninvasive assessment of myocardial elasticity changes by shear wave amplitude variations. *Magn Reson Med*. 2009;61:668–677.
12. Nagueh SF, Appleton CP, Gillebert TC, et al. Recommendations for the evaluation of left ventricular diastolic function by echocardiography. *J Am Soc Echocardiogr*. 2009;22:107–133.
13. Klatt D, Asbach P, Rump J, et al. In vivo determination of hepatic stiffness using steady-state free precession magnetic resonance elastography. *Invest Radiol*. 2006;41:841–848.
14. Asbach P, Klatt D, Hamhaber U, et al. Assessment of liver viscoelasticity using multifrequency MR elastography. *Magn Reson Med*. 2008;60:373–379.
15. Rump J, Klatt D, Braun J, et al. Fractional encoding of harmonic motions in MR elastography. *Magn Reson Med*. 2007;57:388–395.
16. Robert B, Sinkus R, Gennisson JL, et al. Application of DENSE-MR-elastography to the human heart. *Magn Reson Med*. 2009;62:1155–1163.
17. Kolipaka A, McGee KP, Araoz PA, et al. Evaluation of a rapid, multiphase MRE sequence in a heart-simulating phantom. *Magn Reson Med*. 2009;62:691–698.
18. Kolipaka A, McGee KP, Araoz PA, et al. MR elastography as a method for the assessment of myocardial stiffness: comparison with an established pressure-volume model in a left ventricular model of the heart. *Magn Reson Med*. 2009;62:135–140.
19. Gazoti Debessa CR, Mesiano Maifrino LB, de Souza RR, et al. Age related changes of the collagen network of the human heart. *Mech Ageing Dev*. 2001;122:1049–1058.
20. Rossi MA. Pathologic fibrosis and connective tissue matrix in left ventricular hypertrophy due to chronic arterial hypertension in humans. *J Hypertens*. 1998;16:1031–1041.